Paper
Int'l J. of Aeronautical & Space Sci. 16(4), 493–499 (2015)
DOI: http://dx.doi.org/10.5139/IJASS.2015.16.4.493

IJASS
International Journal of Aeronautical and Space Sciences

Numerical Analysis of NACA64-418 Airfoil with Blunt Trailing Edge

Hong-Seok Yoo and Jang-Chang Lee*

Department of Mechanical Engineering, Andong National University, Andong 36729, Republic of Korea

Abstract

The aerodynamic performance of blunt trailing edge airfoils was investigated. The flow fields around the modified NACA64-418, which consists of the tip blade of the wind turbine and Mexico model of IEA wind, were analyzed. To imitate the repaired airfoil, the original NACA64-418 airfoil, a cambered airfoil, is modified by the adding thickness method, which is accomplished by adding the thickness symmetrically to both sides of the camber line. The thickness ratio of the blunt trailing edge of the modified airfoil, t_{TE} /t_{max}, is newly defined to analyze the effects of the blunt trailing edge. The shape functions describing the upper and lower surfaces of the modified NACA64-418 with blunt trailing edge are obtained from the curve fitting of the least square method. To verify the accuracy of the present numerical analysis, the results are first compared with the experimental data of NACA64-418 with high Reynolds number, Re=6×10^6, measured in the Langley low-turbulence pressure tunnel. Then, the aerodynamic performance of the modified NACA64-418 is analyzed. The numerical results show that the drag increases, but the lift increases insignificantly, as the trailing edge of the airfoil is thickened. Re-circulation bubbles also develop and increase gradually in size as the thickness ratio of the trailing edge is increased. These re-circulations result in an increase in the drag of the airfoil. The pressure distributions around the modified NACA64-418 are similar, regardless of the thickness ratio of the blunt trailing edge.

Key words: Aerodynamic performance, Blunt trailing edge airfoil, NACA64-418, Tip blade, Wind turbine

1. Introduction

All countries of the world are interested in the development of alternative energy sources, due to the crisis brought about by the exhaustion of fossil fuels, and are making a lot of investments in the development of green energy technologies. Especially, wind power turbines have come under the spotlight as a favorable recycle energy source. In our country, numerous wind power plant towns have been created and are in operation. Most domestic wind turbines have been operated for more than ten years. After such a long employment period, the tip blades become cracked and are repaired through maintenance in order to allow their continuous use, as shown in Fig. 1. These resulting thickened and modified shapes of the tip blades cause them to make some noise and have an effect on their aerodynamic characteristics.

Each manufacturing company has its own model of wind turbine blade. Especially, the Mexico model of IEA wind [1] consists of three different types of airfoils for the shape of wind turbine blade. This model adopts the DU91-W250 airfoil at the hub blade, RISO-A1-21 airfoil at the middle blade, and NACA64-418 airfoil at the tip blade as depicted in Fig. 2. Schepers et al [1] conducted a wind tunnel experiment for the Mexico rotor blade to measure the characteristics of the rotating airfoil.

For the NACA 63 and 64 6-digit series of airfoils, which are being used in the wind turbine blades, Timmer [2] measured the 2-D aerodynamic characteristics in a Langley low-turbulence pressure tunnel. The maximum lift and drag coefficients of the NACA63-x18 and NACA64-x18 airfoils, whose maximum thickness ratio is 18%, are measured at high Reynolds numbers, Re=6×10^6 and Re=9×10^6, for various angles of attack, -8^o < α < 20^o. The results are compared with the numerical analysis of RFOIL which is a modified version

* Professor, Corresponding author: leejc@andong.ac.kr

Received: July 27, 2015 Revised: December 21, 2015 Accepted: December 22, 2015

http://ijass.org pISSN: 2093-274x eISSN: 2093-2480

of XFOIL.

Summer and Page [3] investigated the lift and moment characteristics of a 10-percent-thick circular-arc airfoil in the wind tunnel when the thickness ratio of the blunt trailing edge, h/t, is changed, where h is the thickness of the trailing edge and t is the maximum thickness of the airfoil. For $0 < h/t < 1$, the changes in the aerodynamic performance of the thickened circular-arc airfoil are studied for Mach numbers in the range from 0.3 to 0.9 for various angles of attack, $-10^o < \alpha < 10^o$. For a fairly well thickened blunt trailing edge, the drag shows a large value because of the Karman vortex-street appearing in the wake region.

Smith and Schaefer [4] explore the 2-D aerodynamic characteristics of three modified NACA0012 airfoils in the wind tunnel. These airfoils are made by cutting off 1.5%, 4%, and 12.5% of the original chord from the trailing edge of the NACA0012 airfoil section. The lift, drag, and pitching moment are measured at high Reynolds numbers, $Re=3\times10^6$ and $Re=6\times10^6$, for various angles of attack, $-10^o < \alpha < 20^o$.

In general, the cutting off and adding thickness method are used for creating a blunt trailing edge airfoil [5, 6]. The cutting off method involves truncating the original chord from the trailing edge and rescaling the shortened chord to a unit chord length. The problem with this method is that the value of t/c for the airfoil increases and its camber line changes, as shown in Fig. 3 where t and c are the maximum thickness and chord length of the airfoil, respectively. Therefore, the cutting off method makes it impossible to compare the aerodynamic performance of the resulting airfoils with that of the original airfoil consistently. On the other hand, the adding thickness method involves adding thickness symmetrically to both sides of the camber line, as depicted in Fig. 4. The merit of this method is that, without masking the true effect of the blunt trailing edge, through the combination of the modified camber line and increased maximum thickness, the effect of the blunt trailing edge alone can be considered and accounted for.

Fig. 1. Damaged and repair tip blade of wind turbine [9].

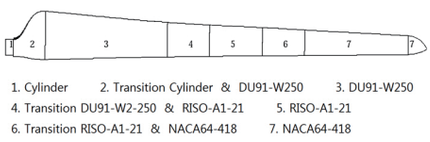

Fig. 2. Maxico rotor blade planform [1].

Standish and van Dam [5] investigated the aerodynamic characteristics of the baseline airfoil, the truncated version (cutting off method), and the blunt trailing edge version (adding thickness method) by numerical analysis. The baseline airfoil, TR-35, has a value of t/c=0.35 with a sharp trailing edge. The truncated airfoil, TR-35.80, is made by cutting off the aft 20% of the TR-35 airfoil and is then rescaled to a unit chord length. This process results in values of t/c=43.6% and t_{TE}/c=10.1% for the TR-30.80 airfoil, where t_{TE} is the thickness of the blunt trailing edge. The blunt trailing edge airfoil, TR-35-10, is made by adding the thickness symmetrically to both sides of the camber line of the TR-35 airfoil. This airfoil has values of t/c=0.35 and t_{TE}/c=0.1.

Murcia and Pinilla [6] also produce twenty modified versions of the NACA 4421 airfoil, which were created by the cutting off and adding thickness methods, i.e. NACA 7724 R 15 airfoil (cutting off method) and NACA 4221 ξ (0.5) 15 airfoil (adding thickness method). The aerodynamic performances of these airfoils were studied by ANSYS CFX. The result showed that the adding thickness method produces larger maximum lift and critical angles of attack than the cutting off method.

In above such researches, the high Reynolds number is used to investigate aerodynamic characteristics of airfoils. However, the wind speed is limited to analyze an airfoil used in wind turbine. There are two wind speeds to produce a power in wind turbine, cut-in wind speed(minimum wind speed) and cut-out wind speed(maximum wind speed), respectively. The cut-in wind speed is the initial speed producing the power(i.e. 3m/s~5m/s) and the cut-out wind speed is the limited speed preventing the component demolition. The 3MW wind turbine of Acciona Windpower[10] and the WinDS3000 developed by Doosan heavy industry[11] which is the offshore wind turbine have a cut-out wind speed of 25m/s. The 5MW offshore wind turbine[12, 13] has a cut-out wind speed of 30m/s. The general cut-off wind speed as a representative characteristic of the

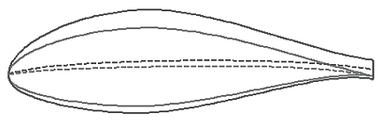

Fig. 3. Cutting off method.

Fig. 4. Adding thickness method.

DOI: http://dx.doi.org/10.5139/IJASS.2015.16.4.493

turbine is a speed between 10m/s and 15m/s which is the optimal wind speed for the wind turbine is recommended.

In this study, the 2-D aerodynamic performances of modified NACA64-418 airfoils with a blunt trailing edge are investigated. These airfoils are obtained by the adding thickness method and are imitated for the purpose of repairing the damaged tip blade of the wind turbine, as shown in Fig. 1. In order to analyze the effects of the blunt trailing edge of the modified NACA64-418 airfoils, the thickness ratio of the blunt trailing edge, t_{TE}/t_{max}, is newly defined, where t_{TE} is the thickness of the blunt trailing edge and t_{max} is the maximum thickness of the airfoil, as depicted in Fig. 5. Here, the t_{max} value of the modified airfoil obtained through the adding thickness method is unchanged and remains a constant. Therefore, it can be used as the reference length of the modified NACA64-418 airfoil. Again, airfoils from the NACA 63 and 64 six-digit series are still being used in wind turbine blades today[2]. The Mexico model of IEA wind adopts the NACA64-418 airfoil as the tip blade just in time. Timmer[2] provides the experimental data for NACA63-x18 and NACA64-x18 airfoils. These experimental data are used for verifying the accuracy of present numerical analysis.

2. Numerical Method

2.1 Governing equations

The Reynolds-averaged Navier Stokes equations can be used with approximations based on knowledge of the properties of flow turbulence to give approximate time-averaged solutions to the Navier-Stokes equations. The conservative forms of governing equations are as follows [7]:

Continuity:

$$\rho\frac{\partial}{\partial x_i}(u_i) = 0 \tag{1}$$

Momentum:

$$\rho\frac{\partial}{\partial t}(u_i) + \rho\frac{\partial}{\partial x_j}(u_i u_j) = -\frac{\partial p}{\partial x_i} + \frac{\partial}{\partial x_j}\left[\mu\left(\frac{\partial u_i}{\partial x_j}+\frac{\partial u_j}{\partial x_i}-\frac{2}{3}\delta_{ij}\frac{\partial u_l}{\partial x_l}\right)\right] + \frac{\partial}{\partial x_j}\left(-\rho\overline{u'_i u'_j}\right) \tag{2}$$

For variable-density flows, Equation (1) and (2) can be interpreted as Favre-averaged Navier-Stokes equations, with the velocities representing the mass-averaged values, but this case assumed incompressible flow. The modeled energy equation is,

$$\rho\frac{\partial}{\partial t}(E) + \nabla\cdot\left(\vec{v}(\rho E + p)\right) = \nabla\cdot\left(k_{eff}\nabla T - \sum_j h_j\vec{J}_j + \left(\bar{\bar{\tau}}_{ij}\cdot\vec{v}\right)\right) \tag{3}$$

where E and T are the mass-averaged values and $(\bar{\bar{\tau}}_{ij})$ is the stress tensor, defined as

$$\bar{\bar{\tau}}_{ij} = \mu_{eff}\left[\left(\frac{\partial u_i}{\partial x_j}+\frac{\partial u_j}{\partial x_i}\right)-\frac{2}{3}\frac{\partial u_k}{\partial x_k}\delta_{ij}\right] \tag{4}$$

The term $\bar{\bar{\tau}}_{ij}$ is the viscous heating due to the dissipation.

The transport equations for the transition SST model used in the present work is based on the Wilcox k-ω model, is good to predict the transition point [8].

The equations governing the turbulence kinetic energy and specific dissipation rate are

$$\rho\frac{\partial}{\partial t}(k) + \rho\frac{\partial}{\partial x_i}(ku_i) = \frac{\partial}{\partial x_j}\left(\Gamma_k\frac{\partial k}{\partial x_j}\right) + G_k^* - Y_k^* \tag{5}$$

$$G_k^* = \gamma_{eff}\tilde{G}_k, \qquad Y_k^* = min\left(max\left(\gamma_{eff}, 0.1\right), 1.0\right)Y_k \tag{6}$$

$$\rho\frac{\partial}{\partial t}(\omega) + \rho\frac{\partial}{\partial x_i}(\omega u_j) = \frac{\partial}{\partial x_j}\left(\Gamma_\omega\frac{\partial\omega}{\partial x_j}\right) + G_\omega - Y_\omega + D_\omega \tag{7}$$

where $\tilde{G}_k$ and Y_k are the original production and destruction terms for the SST model. The term $\tilde{G}_k$ represents the generation of turbulence kinetic energy due to mean velocity gradients. Γ_k and Γ_ω represent the effective diffusivity of k and ω. Y_k and Y_ω represent the dissipation of turbulence kinetic energy, and is defined in a similar manner as in the standard k-ω model.

2.2 Design of airfoil

As mentioned above, the shape of the repaired airfoil becomes that of a blunt trailing edge airfoil (see Fig. 1). The surface curve line of this modified airfoil is designed by the adding thickness method. The shape functions describing the upper and lower surface of the modified NACA64-418 are obtained from the curve fitting of the least square method with the commercial program, Maple. The values of t_{TE}/t_{max} are assumed to be 10%, 20%, and 30% for the purpose of describing the shape of the repaired airfoil. The equation of the surface curve line is fitted with the 8th and 10th polynomials for the upper and lower surfaces, respectively, as follows;

$$y_u = a_0 + a_1X + a_2X^2 + a_3X^3 + a_4X^4 + a_5X^5 + a_6X^6 + a_7X^7 + a_8X^8 \tag{8}$$

$$y_1=b_0+b_1x+b_2x^2+b_3x^3+b_4x^4+b_5x^5+ b_6x^6+b_7x^7+b_8x^8+b_9x^9+b_{10}x^{10} \quad (9)$$

The NACA64-418 airfoil is an asymmetry and cambered airfoil. The lower surface has more complex shape than the upper surface shape near the trailing edge(see the original shape at Fig. 5). The lower surface of original airfoil is well fitted with higher order polynomials (i.e. 10th order).

The values of coefficients in the above polynomial equations for various values of t_{TE}/t_{max} are listed in tables 1 and 2.

Again, the maximum thickness t_{max} of the NACA64-418 airfoil is 18% of the chord and is located at 37% of the chord. This airfoil is an asymmetry and cambered airfoil (see Fig. 5).

2.3 Numerical results and discussions

For the numerical analysis in this study, the commercial program Pointwise is used for the shape modeling and grid generation and ANSYS Fluent is used for carrying out the aerodynamic analysis.

The flow field around the NACA64-418 airfoil is assumed to be a 2-D steady incompressible viscous flow and C-type structured grids were used for the various airfoils with sharp trailing edge and blunt trailing edges. All of the grids are constructed with the far field at a distance of 15 chord lengths.

Table 1. Upper surface coefficients.

	10%	20%	30%
a_0	0.144237367	0.144437367	0.144637367
a_1	1.976929270	1.976929270	1.976929270
a_2	-5.879740658	-5.879740658	-5.879740658
a_3	8.936912491	8.936912491	8.936912491
a_4	-8.184608171	-8.175607121	-8.166606071
a_5	5.472917239	5.472917239	5.472917239
a_6	-4.411729525	-4.411729525	-4.411729525
a_7	3.289268782	3.289268782	3.289268782
a_8	-1.046711011	-1.046511011	-1.046311011

Table 2. Lower surface coefficients.

	10%	20%	30%
b_0	0.02279410262	0.02299410262	0.02319410262
b_1	-0.5656443195	-0.5656443195	-0.5656443195
b_2	0.9120746550	0.9120746550	0.9120746550
b_3	0.04149831968	0.04149831968	0.04149831968
b_4	-0.3148582423	-0.3238592923	-0.3328603423
b_5	-0.8675082292	-0.8675082292	-0.8675082292
b_6	0.9564599354	0.9564599354	0.9564599354
b_7	-0.2661621417	-0.2661621417	-0.2661621417
b_8	0.6757313362	0.6757313362	0.6757313362
b_9	-0.8112075037	-0.8112075037	-0.8112075037
b_{10}	0.2078210375	0.2078210375	0.2078210375

The pressure and temperature of the air are assumed to be 1 atm and 288.15 K as sea level conditions, respectively. As the boundary conditions, the pressure outlet and velocity inlet condition are selected. Also, the pressure based condition, implicit method, and least-square cell based condition are adopted. The second order upwind scheme is selected as the spatial differencing method and Roe-FDS as the flux type. As the turbulence model, the Transition SST four equation model is adopted and the turbulence intensity is set to 0.1 %. In order for the wall y^+ value to be less than one, the first grid size is set to 4.5×10^{-6}. The number of grids used in this study is 50,000.

Figure 5 shows the original NACA64-418 airfoil with the sharp trailing edge and the modified NACA64-418 airfoil with various trailing edge thickness-to-maximum thickness-ratios, t_{TE}/t_{max}, which are assumed to be 10%, 20%, and 30% created by the adding thickness method. As t_{TE}/t_{max} is increased, the intersection between the adding line and the surface of the original airfoil moves to the position of the maximum thickness t_{max}.

In Fig. 6, the C-type grids around the NACA64-418 airfoil are represented. The dense grids are distributed in the boundary layer, the trailing edge, and the wake region. Since the wake region of the blunt trailing edge would be expected to develop more complicated flow, such as a reverse pressure gradient, the use of dense grids is imposed.

To verify the accuracy of the numerical analysis, the lift and the lift-drag results compared with the wind tunnel experiment of Timmer [2] for various angles of attack, $-10^o < \alpha < 20^o$, are represented in Figs. 7-8. Since the experiment is

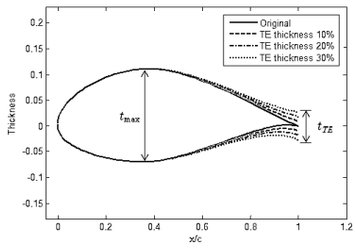

Fig. 5. Airfoils with ratios (t_{TE}/t_{max}) of 10%, 20%, and 30% and the original NACA64-418 airfoil with t_{max} = 18%.

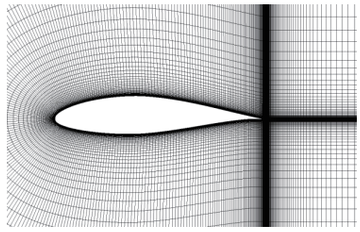

Fig. 6. C-type structured grids around NACA64-418 airfoil.

DOI: http://dx.doi.org/10.5139/IJASS.2015.16.4.493

conducted with Re=6×10^6, the corresponding velocity, U_∞=90 m/s, is used as the inlet velocity of this calculation.

In Fig. 7, good agreement is shown between the computed and experimental lift results, especially in the linear region for -8^o < α < 10^o. However, some deviation appears in the stall zone. Such a deviation in the stall zone is also found in a previous study, i.e. Fig. 12 of Timmer[2]. The lift-drag results shown in Fig. 8 represent good agreement between the computed and experimental results. All of the calculations in this paper for the modified NACA64-418 airfoil with the blunt trailing edge are carried out on the basis of this accuracy and use the same flow conditions to determine the effects of the blunt trailing edge on the aerodynamic characteristics.

The lift changes of the original and modified NACA64-418 airfoils with various thickness ratios of the blunt trailing edge, t_{TE}/t_{max}, are shown in Fig. 9 as the angle of attack changes from -10^o to 17^o where an inlet velocity of U_∞=15 m/s is used. The lift values for -10^o < α < 8^o are the same regardless of the thickness ratio of the blunt trailing edge. There is no effect of t_{TE}/t_{max} on the lift, because all of the camber lines of the modified airfoils maintain the same line. However, the lift increases in the zone of high angle of attack as t_{TE}/t_{max} is increased.

Figure 10 shows the lift-drag polar curves of the airfoils for various angles of attack, -10^o < α < 17^o. As t_{TE}/t_{max} is increased, the drags is clearly increased. As mentioned above, the changes of t_{TE}/t_{max} have no effect on the lift for -10^o < α < 8^o, but have a considerable effect on the drag, because the emergence of a reverse pressure gradient at the wake to the rear of the blunt trailing edge results in an increase in the drag (see Fig. 12).

Figure 11 represents the drag changes of the airfoils for all angles of attack with U_∞=15 m/s. The drag undergoes U-type changes. That is, the drag is decreased for -10^o < α < 0^o and is gradually increased above zero degree. It is evident that the drag increases as the trailing edge of the airfoil is thickened.

Figure 12 shows the streamline contours in the wake region with α=8^o according to the thickness-to-maximum thickness-ratio, t_{TE}/t_{max}, for the sharp trailing edge and 10%, 20%, and 30% blunt trailing edges. Here, due to the inertia

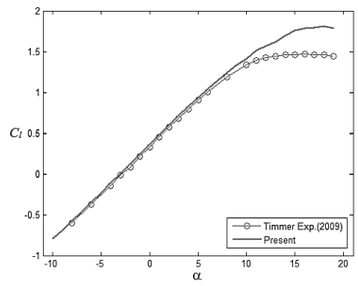

Fig. 7. Expreimental and calculated lift curve for NACA64-418 airfoil with Re=3×10^6 and U_∞=90m/s.

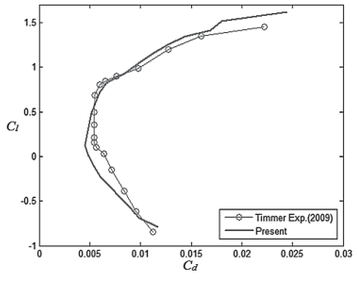

Fig. 8. Experimental and calculated lift-drag curve for NACA64-418 airfoil withRe=3×10^6 and U_∞=90 m/s.

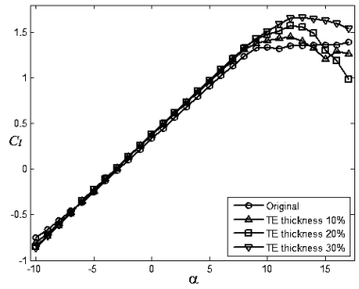

Fig. 9. Lift curves for original and modified NACA64-418 airfoils with U_∞=15 m/s.

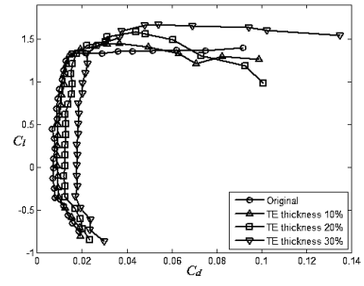

Fig. 10. Lift-Drag polar curves for original and modified NACA64-418 airfoils with U_∞=15 m/s.

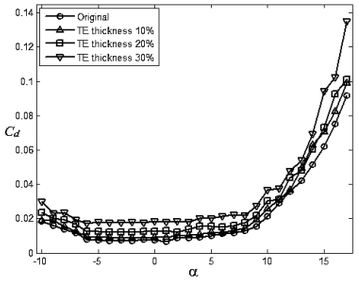

Fig. 11. Drag curves for original and modified NACA64-418 airfoils with U_∞=15 m/s.

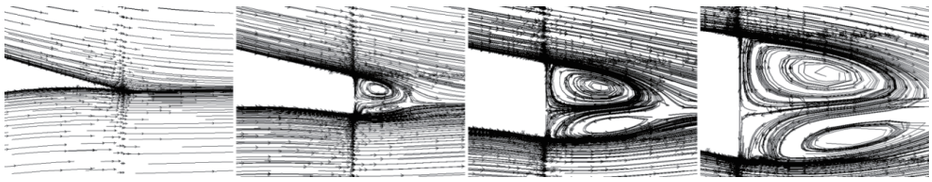

Fig. 12. Development of re-circulation bubbles in the wake region according to t_{TE}/t_{max} with $\alpha = 8^{\circ}$; for sharp trailing edge and 10%, 20%, and 30% blunt trailing edges with U_{∞}=15m/s.

momentum of the leaving flow along the upper surface near the trailing edge, the reversed flow occurs at the blunt trailing edge. Another reversed flow due to the leaving flow along the lower surface occurs. Therefore, the double bubbles exit at the blunt trailing edge. The size of upper bubble is larger than that of lower bubble. This means that the flow velocity along upper surface is faster than that of lower surface. Re-circulation bubbles develop and increase gradually in size as t_{TE}/t_{max} is increased. This re-circulation results in increasing drag.

In Fig. 13, the lift-to-drag ratios of the airfoils are shown for $-10^{o} < \alpha < 17^{o}$. The change of this ratio is reversed at $\alpha = -3^{o}$ as tTE /tmax is increased. That is, the lift-to-drag ratio is increased for $\alpha < -3^{o}$, but is decreased for $-3^{o} < \alpha < 12^{o}$. This change in the angle of attack is caused by the change of drag rather than that of the lift, because the lift linearly increases as the angle of attack increases, but the drag exhibits U-type changes.

Figure 14 represents the pressure distributions around the modified NACA64-418 airfoil, which are similar, regardless of the thickness ratio of the blunt trailing edge. At the trailing edge, there are few changes. This distribution at the trailing edge is due to the effect of the wake region at which more complicate flows develop as the trailing edge of the airfoil is thickened.

In Fig. 15, the pitching moment for the airfoils is shown for $-10^{o} < \alpha < 17^{o}$. The aerodynamic center of an airfoil is usually close to 25% of the chord behind the leading edge of the airfoil. The pitching moment values for $-10^{o} < \alpha < 1^{o}$ are the same regardless of the thickness ratio of the blunt trailing edge, but increases afterward as t_{TE}/t_{max} is increased. Also, the pitching moments for all thickness ratios of the blunt trailing edge linearly increase as the angle of attack is increased, but are suddenly decreased at the stall zone.

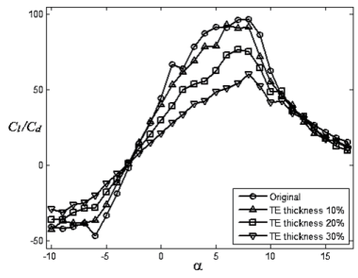

Fig. 13. Lift-to-drag ratio for original and modified NACA64-418 airfoils with U_{∞}=15 m/s.

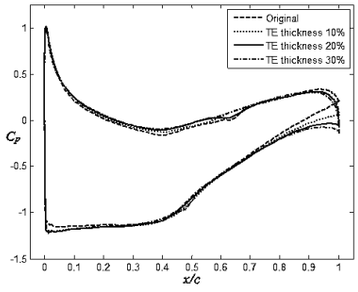

Fig. 14. Pressure distributions around the surface of the original and modified NACA64-418 airfoils with $\alpha = 4^{\circ}$ and U_{∞}=15 m/s.

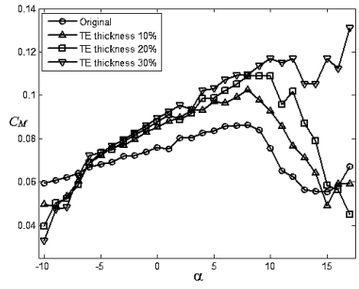

Fig. 15. Moment curves for original and modified NACA64-418 airfoils with U_{∞}=15 m/s.

3. Conclusion

The damaged tip blade of the wind turbine is thickened through the repair process. The modified NACA64-418 airfoil created by the adding thickness method is imitated for the repair airfoil. In this study, the 2-D aerodynamic performances of the airfoil with a blunt trailing edge are investigated according to the thickness ratio of the blunt trailing edge, t_{TE}/t_{max}. The numerical results obtained are as

DOI: http://dx.doi.org/10.5139/IJASS.2015.16.4.493

follows:

1. The drag of the airfoil increase, but the lift increases insignificantly as t_{TE}/t_{max} is increased.
2. The lift-to-drag ratio increases for $\alpha < -3^{o}$ but decreases for $-3^{o} < \alpha < 13^{o}$ as t_{TE}/t_{max} is increased
3. The pressure distributions around the airfoil are similar regardless of t_{TE}/t_{max} except for the trailing edge.

Acknowledgement

This work was supported by a grant from 2015 Research Fund of Andong National University.

References

[1] J. G. Schepers, K. Boorsma, T. Cho, S. Gomez-Iradi, P. Schaffarczyk, A. Jeromin, W. Z. Shen, T. Lutz, K. Meister, B. Stoevesandt, S. Schreck, D. Micallef, R. Pereira, T. Sant, H. A. Madsen, and N. Sorensen, "Final report of IEA task 29, Mexnext(phase 1): Analysis of Mexico wind tunnel measurements," iea wind, 2012. http://www.mexnext.org/resultsstatus.

[2] W. A. Timmer, "An overview of NACA 6-digit airfoil series characteristics with reference to airfoils for large wind turbine blades", *47th AIAA Aerospace Science Meeting*, Orlando, USA, 2009.

[3] J. L. Summers and W. A. Page, "Lift and moment characteristics at subsonic Mach numbers of four 10-percent-thick airfoil sections of varying trailing-edge thickness", Ames Aeronautical Laboratory, California, USA, NACA RM A50J09, 1995.

[4] H. A. Smith and R. F. Schaefer, Aerodynamic characteristics at Reynolds numbers of 3.0x106 and 6x106 of three airfoil sections formed by cutting off various amount from the near portion of the NACA0012 airfoil section, Langley Aeronautical Laboratory, USA, NACA TN 2074, 1950.

[5] K. J. Standish and C. P. van Dam, "Aerodynamic analysis of blunt trailing edge airfoils", *Journal of Solar Energy Engineering*, Vol. 125, 2003, pp. 479-487.

[6] J. P. Murcia and A. Pinilla, "CFD analysis of blunt trailing edge airfoils obtained with several modification methods, Universidad de los Andes", Bogota D.C., Colombia, Rev.ing, ISSN 0121-4993, Enero-junio de, 2011, pp. 14-24.

[7] ANSYS Fluent User's Guide.

[8] F. R. Menter at el, "A correlation based transition model using local variables part 1 – model formulation", *Journal of Turbomachinery*, Vol. 128, No. 3, 2004, pp. 413-42

[9] Rolling Stone Corporation. http://www.rs-corp.co.kr

[10] Acciona Windpower, AW3000 Specifications, ACCIONA Group.

URL: http://www.acciona-windpower.com

[11] Lee K. H. "3MW Offshore Wind Turbine System", *KSME*, 2010, pp. 4498-4511.

[12] J. Jonkman, S. Butterfield, W. Musial and G. Scott, "Definition of a 5-MW Reference Wind Turbine for Offshore System Development", Technical Report NREL/TP-500-38060, 2009.

[13] The University of Edinburgh, Academic Study: Matching Renewable Electricity Generation With Demand: Full Report, Scottish Executive, 2006.